

Supporting Information

Conducting 1D Nanostructures from Light Stimulated Copper Metalated Porphyrin – Dibenzothiophene

Yelukala Rama Krishna,^a Madarapu Naresh,^{a,b} Botta Bhavani,^{a,b} Seelam Prasanthkumar^{*a,b}

^a Polymers & Functional Materials Division, CSIR-Indian Institute of Chemical Technology, Hyderabad-500007, T.S., India.

^bAcademy of Scientific and Innovative Research (AcSIR), Ghaziabad 201002, India

Email of corresponding (*) E-mail: prasanth@iict.res.in (ORCID: 0000-0001-6287-1977)

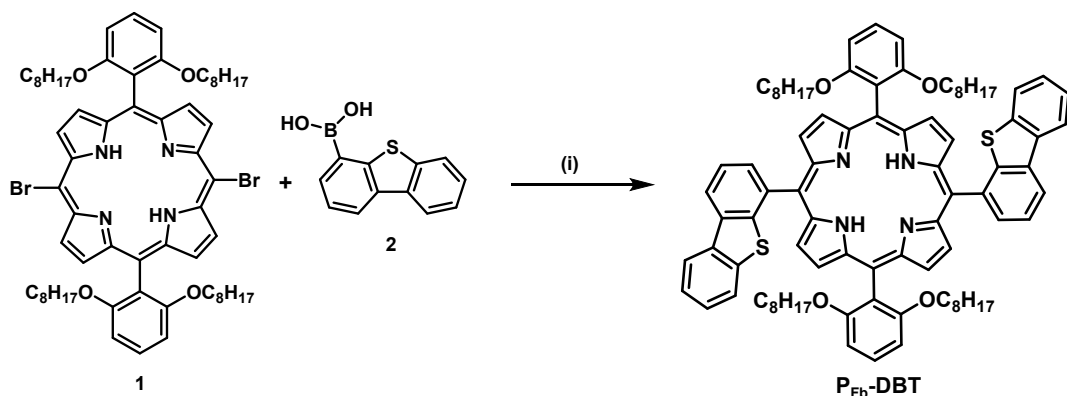
Supporting information

Table of contents

1. Synthesis of P_{Fb}-DBT , P_{Cu}-DBT and P_{Zn}-DBT	S3-S5
2. ¹ H NMR Spectra	S5-S6
3. ¹³ C NMR Spectra.....	S7
4. MALDI-TOF-MS Spectra.....	S8-S9
5. Theoretical calculations of P-DBT derivatives.....	S9
6. Photophysical data of P_{Fb}-DBT and P_{Zn}-DBT	S9-S11
7. MALDI-TOF-MS of light stimulated P-DBT derivatives.....	S11
8. Spectroelectrochemistry of P_{Fb}-DBT	S12
9. Electron microscopic images of P_{Fb}-DBT	S12
10. Electrochemical Impedance analysis of P_{Fb}-DBT and P_{Cu}-DBT at before and light illuminations conditions.....	S13-S15

1. Synthesis of P_{Fb}-DBT, P_{Cu}-DBT and P_{Zn}-DBT

1.1. Synthesis of P_{Fb}-DBT:

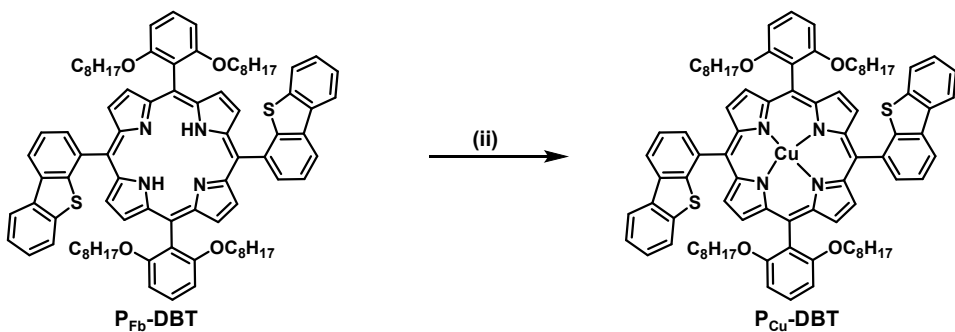


Scheme S1. Reagent and Conditions: (i) Pd(PPh₃)₂Cl₂, Na₂CO₃, THF, Toluene, 90 °C, 12 h, N₂ atmosphere, yield: 60%.

Synthetic Procedure for P_{Fb}-DBT: To a 5 mL THF solution of dibromoporphyrin (500 mg, 0.537 mmol), dibenzo[b,d]thiophen-2-ylboronic acid (1) (1160 mg, 2.296 mmol) in 20 mL toluene, 1M Na₂CO₃ and bis(triphenylphosphine)palladium(II) dichloride Pd(PPh₃)₂Cl₂ (catalytic amount) were added and refluxed for 12 h at 70 °C under N₂ atmosphere. Subsequently, the reaction mixture was washed with ethyl acetate/water and organic layer was separated and dried over sodium sulphate. The crude product was purified by column chromatography (silica gel 100 – 200 mesh, DCM/hexane to give purple solid P_{Fb}-DBT (yield: 60%).

¹H NMR (400 MHz, CDCl₃) δ: 8.69 – 8.39 (m, 9H), 8.30 – 8.06 (m, 4H), 7.76 (s, 2H), 7.55 – 7.33 (m, 6H), 6.81 (s, 3H), 4.00 (s, 1H), 3.74 (d, *J* = 31.5 Hz, 8H), 1.51 (s, 1H), 1.28 (d, *J* = 15.5 Hz, 2H), 1.17 (s, 8H), 0.94 – 0.67 (m, 17H), 0.59 – 0.39 (m, 33H), -2.61 (d, *J* = 53.9 Hz, 2H). ¹³C NMR (126 MHz, CDCl₃) δ: 160.13, 145.64, 140.98, 137.81, 135.64, 135.05, 132.67, 130.99, 130.50, 129.95, 126.70, 124.43, 123.72, 122.86, 122.15, 121.13, 120.40, 116.01, 113.01, 105.07, 68.65, 67.90, 38.75, 31.55, 30.40, 29.66, 29.34, 29.05, 25.38, 23.78, 23.10, 22.82, 22.33, 14.21, 13.95, 11.04. MALDI-TOF-MS (m/z) = 1339.67 (calculated mass = 1339.763).

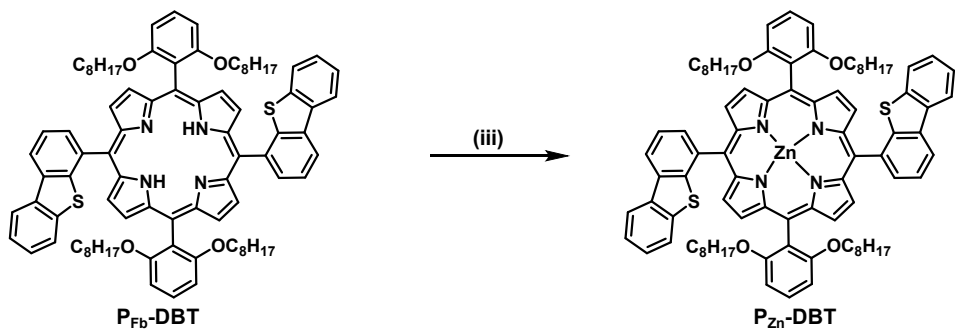
1.2. Synthesis of $\text{P}_{\text{Cu}}\text{-DBT}$:



Scheme S2. Reagent and Conditions: (ii) $\text{Cu}(\text{OAc})_2$, DCM/MeOH (1:3 v/v), 3 h, 25 °C, N_2 atmosphere, yield: 70%.

Synthetic Procedure for $\text{P}_{\text{Cu}}\text{-DBT}$: A mixture of $\text{P}_{\text{Fb}}\text{-DBT}$ (200 mg, 0.00142 mmol) and $\text{Cu}(\text{OAc})_2$ (261 mg, 0.0023 mmol) in DCM/CH₃OH (1:3 v/v) were refluxed for 3 h under N_2 atmosphere at 25 °C. The progress of the reaction monitored by thin layer chromatography (TLC) and excess solvent was removed under reduced pressure. The extraction performed with hexane/DCM. The organic layer was washed with water and dried over Na_2SO_4 . The solid residue was subjected to column chromatography (silica gel: 100–200 mesh, DCM/hexane) to give pink coloured solid (yield: 70%); (MALDI-TOF-MS (m/z) = 1399.67 (calculated mass = 1399.62)).

1.3. Synthesis of $\text{P}_{\text{Zn}}\text{-DBT}$:



Scheme S2. Reagent and Conditions: (iii) $\text{Zn}(\text{OAc})_2$, DCM/MeOH (1:3 v/v), 3 h, 25 °C, N_2 atmosphere, yield: 70%.

Synthetic Procedure for $\text{P}_{\text{Zn}}\text{-DBT}$: The synthetic strategy followed the $\text{P}_{\text{Cu}}\text{-DBT}$ procedure by simple modification of $\text{Cu}(\text{OAc})_2$ with $\text{Zn}(\text{OAc})_2$.

¹H NMR (400 MHz, CDCl₃) δ: 8.70 (dd, *J* = 23.3, 10.5 Hz, 6H), 8.42 (d, *J* = 7.8 Hz, 1H), 8.27 – 8.11 (m, 3H), 7.76 (dd, *J* = 11.8, 7.3 Hz, 2H), 7.49 (t, *J* = 8.2 Hz, 2H), 7.35 (dd, *J* = 19.3, 7.6 Hz, 3H), 7.25 – 7.15 (m, 2H), 6.83 (d, *J* = 8.3 Hz, 3H), 6.39 (t, *J* = 8.1 Hz, 1H), 3.91 – 3.60 (m, 8H), 1.78 – 1.48 (m, 2H), 1.28 (d, *J* = 1.8 Hz, 3H), 1.17 (t, *J* = 3.8 Hz, 12H), 0.95 – 0.74 (m, 12H), 0.54 – 0.31 (m, 33H). ¹³C NMR (101 MHz, CDCl₃) δ: 158.93, 150.83, 150.00, 149.74, 148.07, 145.85, 144.58, 141.67, 139.74, 137.38, 135.09, 134.52, 134.07, 133.74, 131.42, 130.56, 129.86, 129.39, 128.65, 125.45, 123.63, 123.44, 123.44, 123.06, 122.46, 121.62, 120.98, 120.49, 119.64, 117.82, 115.83, 114.83, 112.51, 105.13, 104.07, 103.19, 68.32, 68.13, 66.76, 37.59, 34.80, 33.20, 30.65, 30.33, 29.25, 28.90, 28.16, 27.51, 24.95, 24.19, 22.62, 21.78, 21.15, 13.07, 12.76, 9.88. (MALDI-TOF-MS (m/z) = 1401.67 (calculated mass = 1401.62).

2. ¹H NMR Spectra

2.1. ¹H NMR of P_{Fb}-DBT:

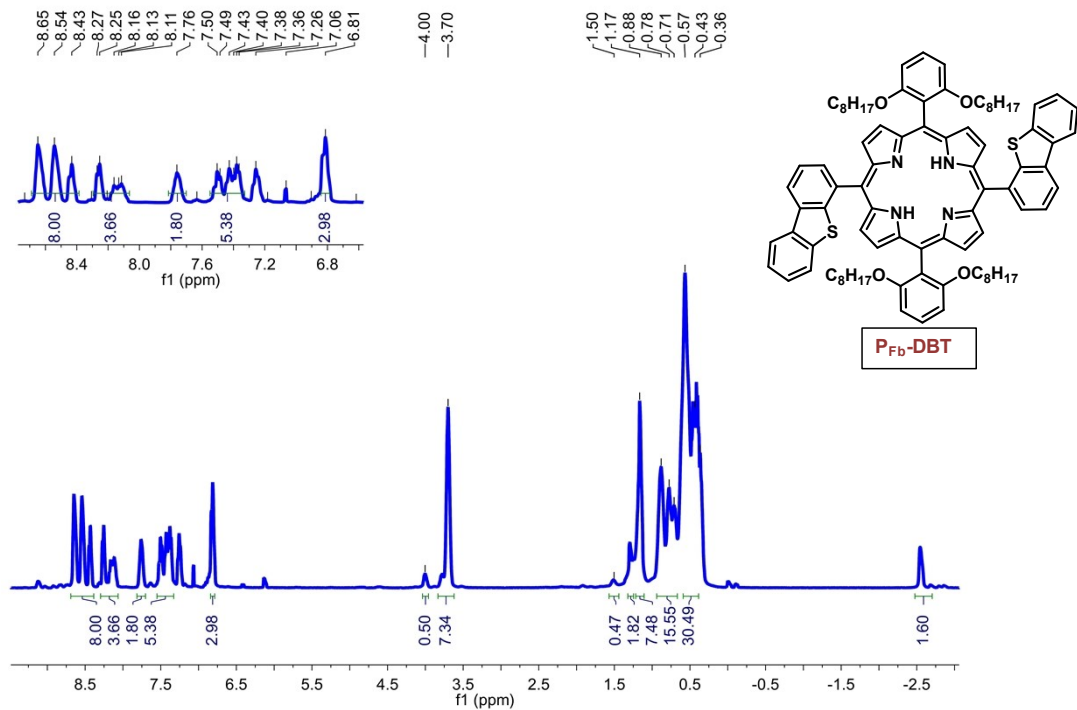


Figure S1. ¹H NMR Spectrum of P_{Fb}-DBT.

2.2. ^1H NMR of $\text{P}_{\text{Zn}}\text{-DBT}$:

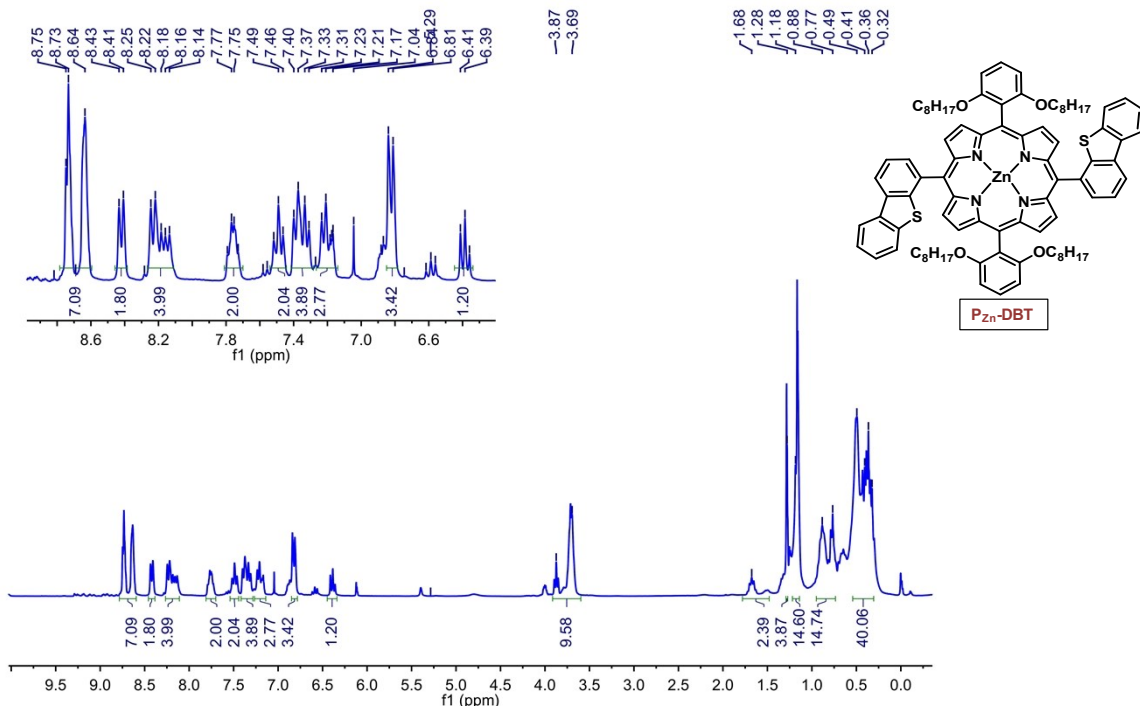


Figure S2. ^1H NMR Spectrum of $\text{P}_{\text{Zn}}\text{-DBT}$.

3. ^{13}C NMR Spectra

3.1. ^{13}C NMR of $\text{P}_{\text{Fb}}\text{-DBT}$:

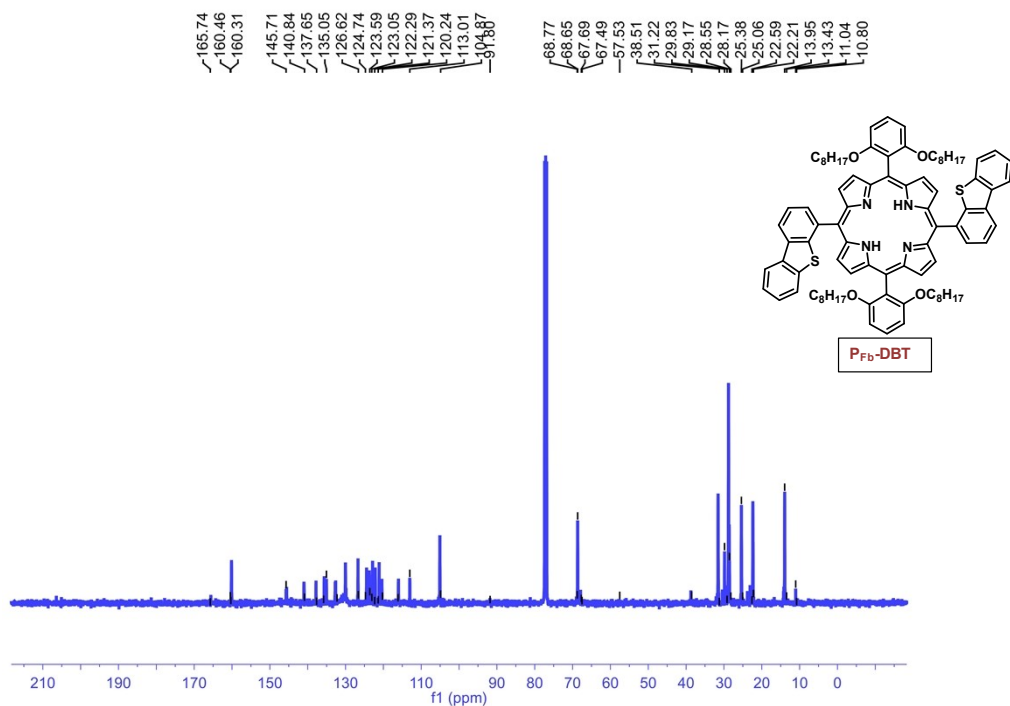


Figure S3. ^{13}C NMR Spectrum of $\text{P}_{\text{Fb}}\text{-DBT}$.

3.2. ^{13}C NMR of $\text{P}_{\text{Zn}}\text{-DBT}$:

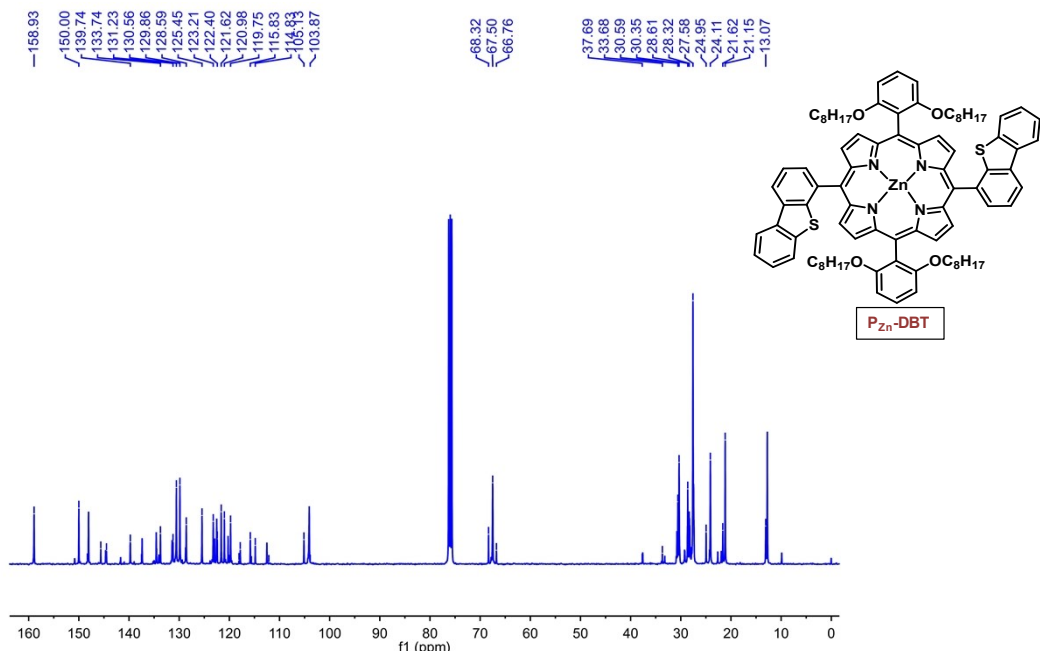


Figure S4. ^{13}C NMR Spectrum of $\text{P}_{\text{Zn}}\text{-DBT}$.

4. MALDI-TOF-MS Spectra

4.1. MALDI-TOF-MS of $\text{P}_{\text{Fb}}\text{-DBT}$:

MALDI-TOF-MS (m/z) = 1339.67 (calculated mass = 1339.763).

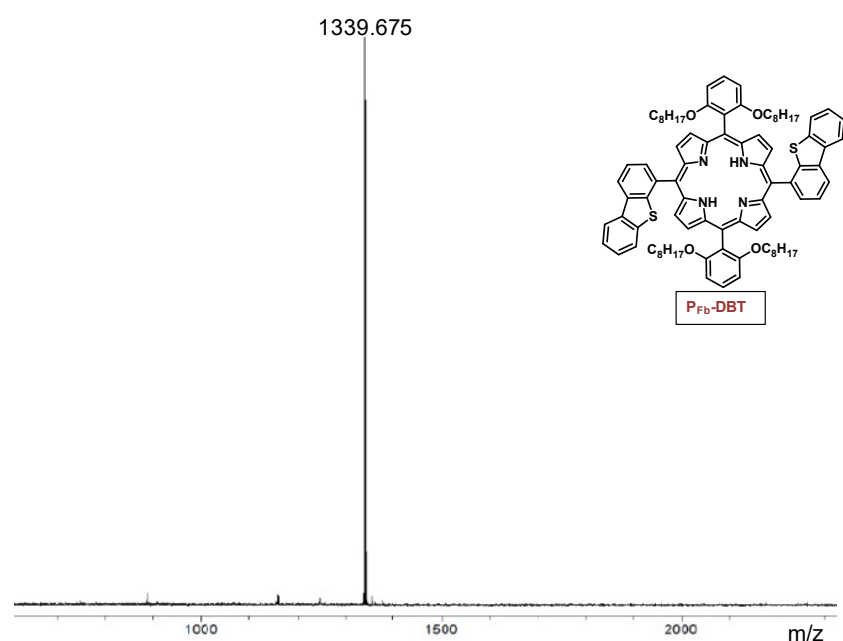


Figure S5. MALDI-TOF-MS Spectrum of $\text{P}_{\text{Fb}}\text{-DBT}$.

4.2. MALDI-TOF-MS of P_{Zn}-DBT:

(MALDI-TOF-MS (m/z) = 1401.67 (calculated mass = 1401.62)).

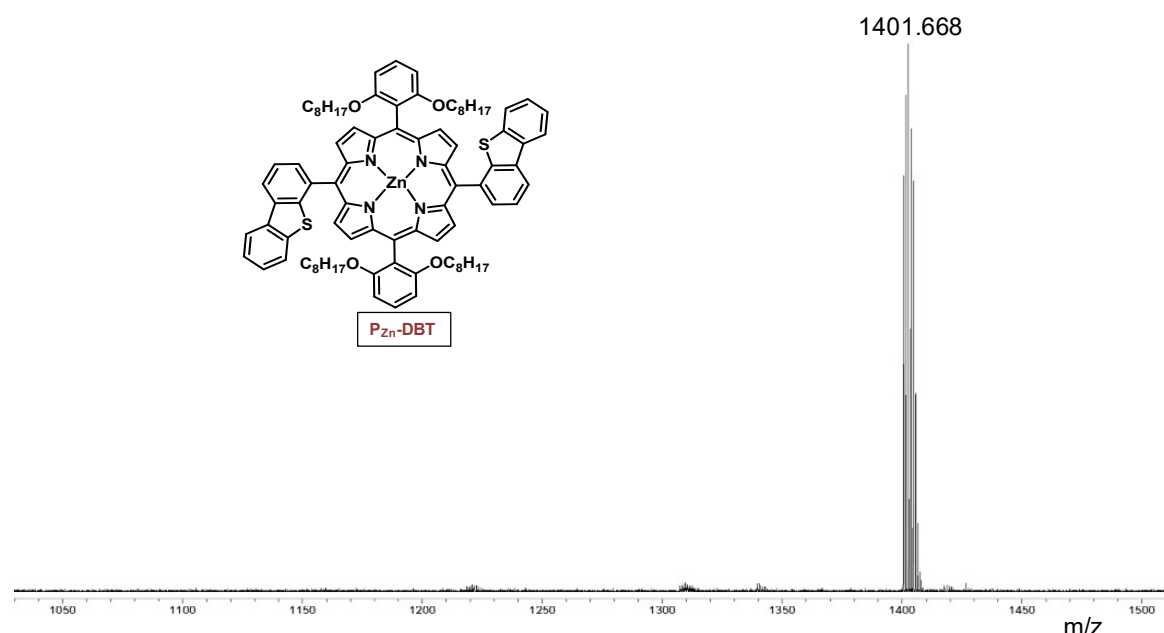


Figure S6. MALDI-TOF-MS Spectrum of P_{Zn}-DBT.

4.3. MALDI-TOF-MS of P_{Cu}-DBT:

(MALDI-TOF-MS (m/z) = 1399.67 (calculated mass = 1399.62)).

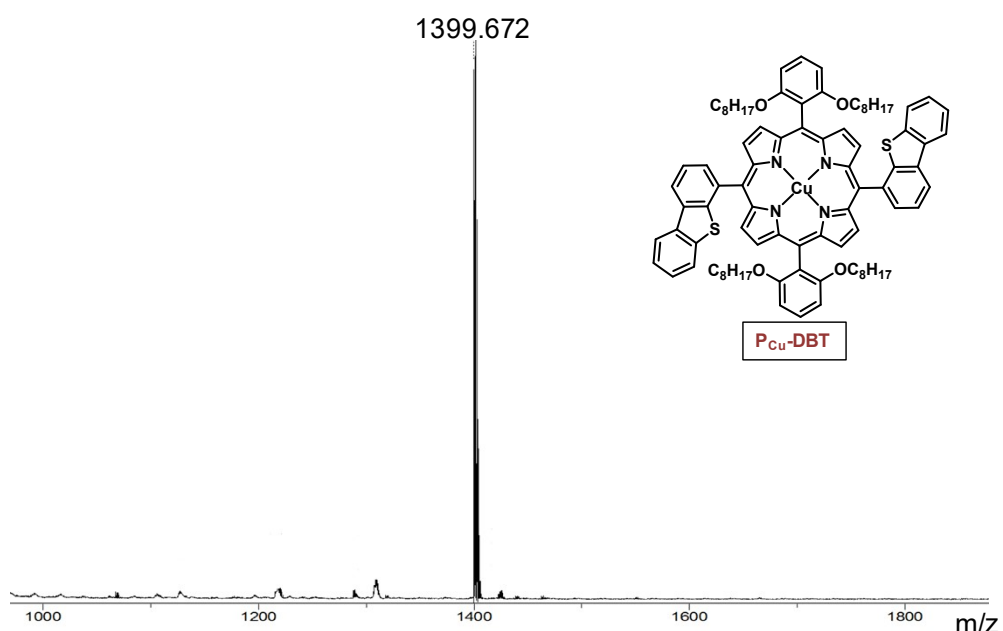


Figure S7. MALDI-TOF-MS Spectrum of P_{Cu}-DBT.

5. Theoretical calculations of P-DBT derivatives:

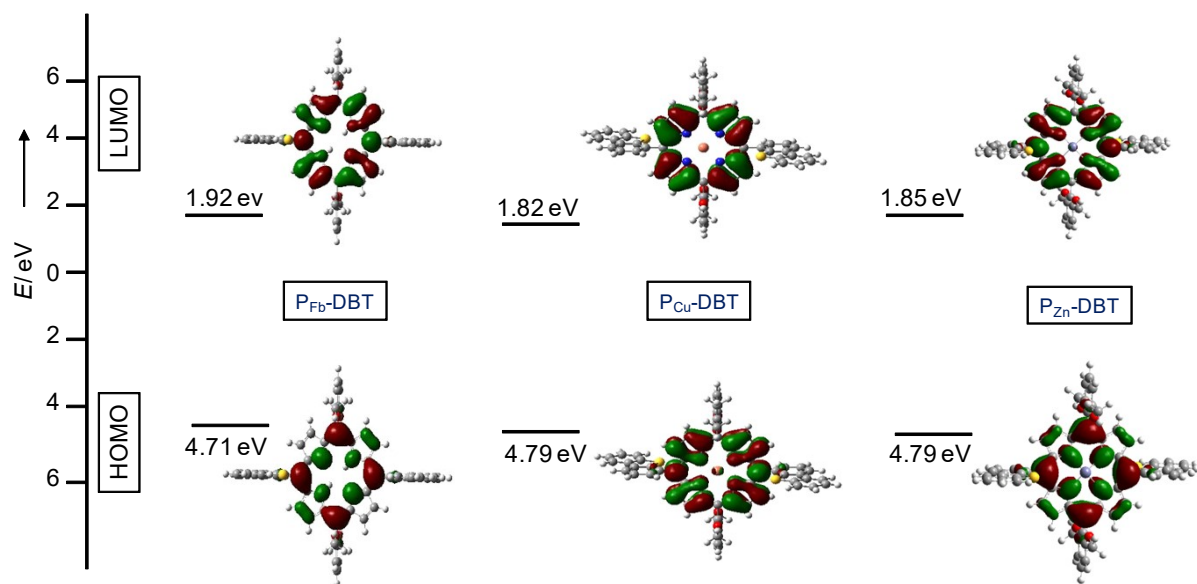


Figure S8. Theoretiecal calculations of **P_{Fb}-DBT**, **P_{Cu}-DBT** and **P_{Zn}-DBT** and their HOMO and LUMO energy levels.

6. Photophysical data of freebase and metalated P-DBT derivatives:

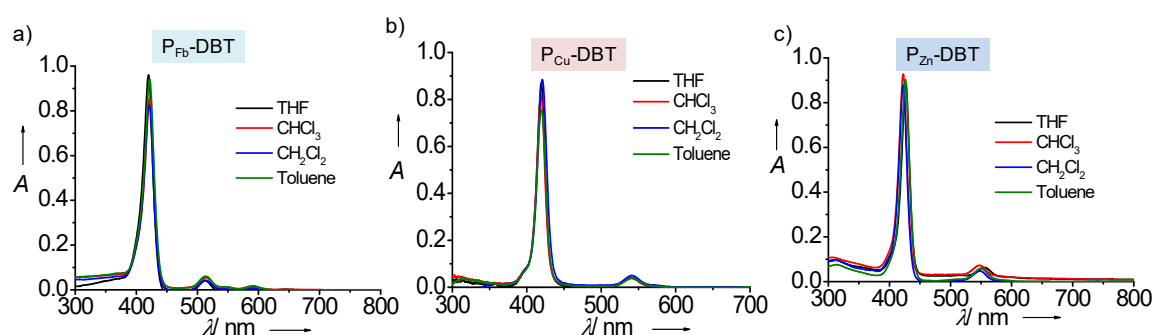


Figure S9. UV-vis optical absorption spectra of a) **P_{Fb}-DBT**, b) **P_{Cu}-DBT** and c) **P_{Zn}-DBT** in various solvents such as tetrahydrofuran (THF), chloroform (CHCl₃), dichloromethane (CH₂Cl₂) and toluene at a concentration of 1×10^{-4} M at 25 °C.

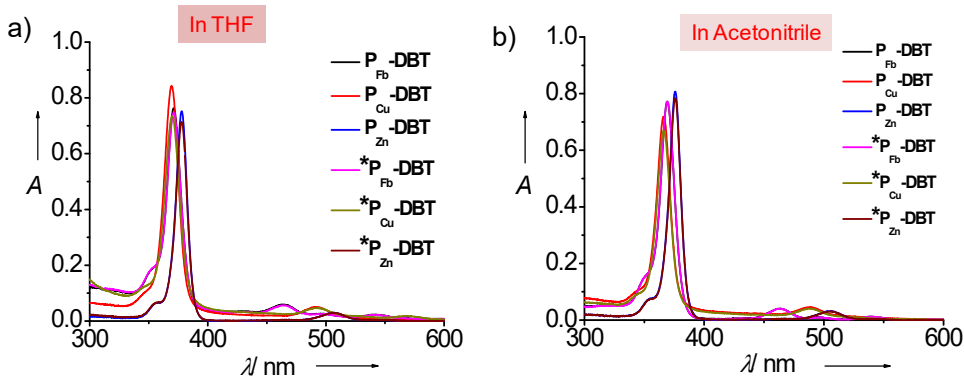


Figure S10. UV-vis optical absorption spectra of P_{Fb} -DBT, P_{Cu} -DBT and P_{Zn} -DBT in tetrahydrofuran (THF) and acetonitrile (ACN) at a concentration of 1×10^{-4} M at 25°C .

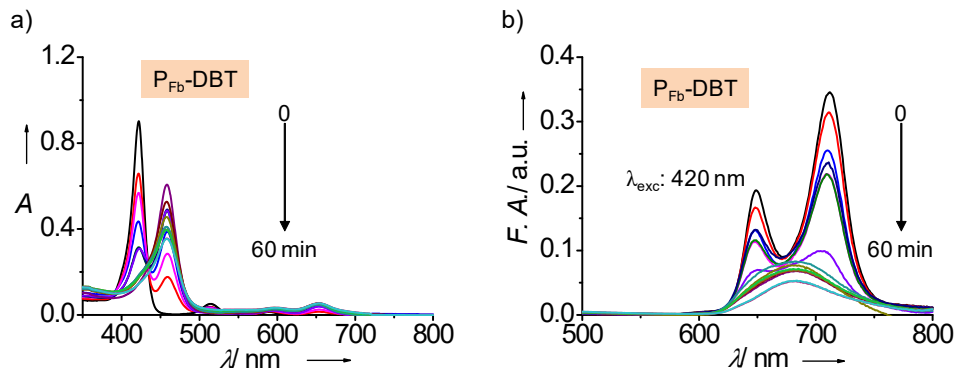


Figure S11. a) UV-vis optical absorption spectra of P_{Fb} -DBT in chloroform with different interval of time from 0 to 60 min at 25°C . b) The corresponding emission spectra of P_{Fb} -DBT at an excitation wavelength of 420 nm.

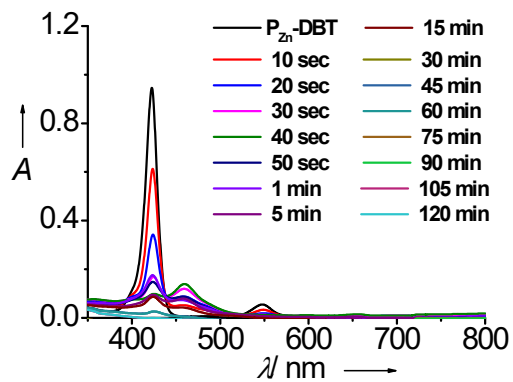


Figure S12. UV-vis optical absorption spectra of P_{Zn} -DBT in chloroform with different interval of time from 0 to 120 min at 25°C .

Table S1. Photophysical and electrochemical data of **P-DBT** derivatives

S.No.	Samples	Absorption		Emission		Lifetime		E_{ox}	E_{red}		
		$\lambda_{\text{max}} \text{ (nm)}$		$\lambda_{\text{ems}} \text{ (nm)}$		$\tau \text{ (ns)}$					
		Before	After light	Before	After light	Before	After light				
1	P_{Fb}-DBT	421	457	728	8.41	4.48	1.302	-0.995			
		514	597			8.70					
		589	652								
2	P_{Cu}-DBT	419	425	-	-	-	0.84	-0.983			
		540				1.36					
3	P_{Zn}-DBT	422	423	668	2.89	0.64	0.66	-1.01			
		547	460			3.48	1.22				

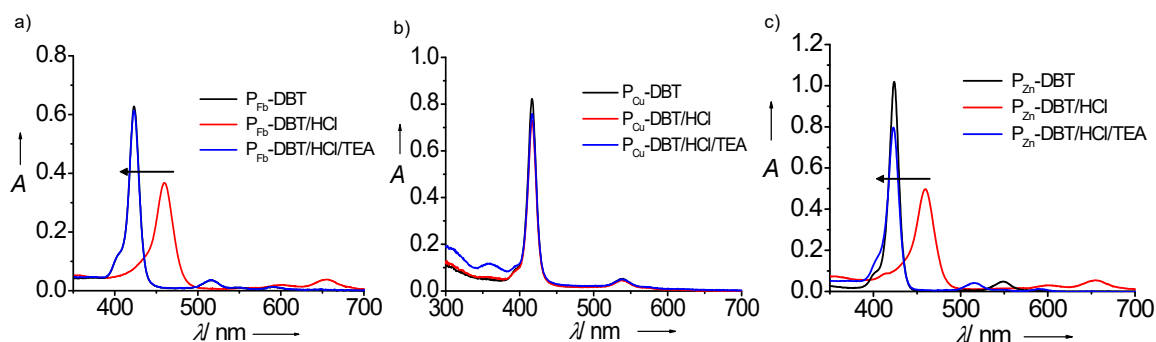


Figure S13. UV-vis optical absorption spectra of a) **P_{Fb}-DBT**, b) **P_{Cu}-DBT** and c) **P_{Zn}-DBT** in tetrahydrofuran and recorded their spectral changes whilst addition of acid and base.

7. MALDI-TOF-MS of light stimulated P-DBT derivatives:

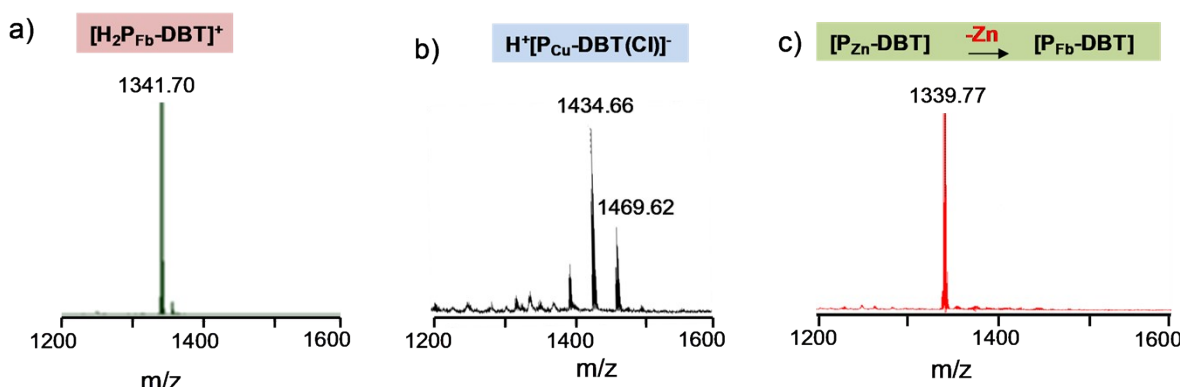


Figure S14. MALDI-TOF-MS spectra of light stimulated samples: a) $[\text{H}_2\text{P}_{\text{Fb}}\text{-DBT}]^+\text{Cl}^-$, b) $\text{H}^+[\text{P}_{\text{Cu}}\text{-DBT}(\text{Cl})]^-$ and c) $\text{P}_{\text{Fb}}\text{-DBT}$.

8 . Spectroelectrochemistry of **P_{Fb}-DBT**:

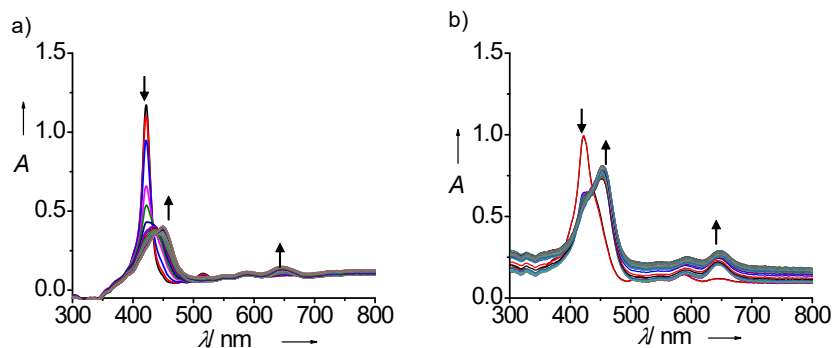


Figure S15. Spectroelectrochemical UV-vis optical absorption spectra of **P_{Fb}-DBT** in chloroform: a) oxidation potential (1.30 V) and b) reduction potential (-1.01 V).

9. Electron microscopic images of **P_{Fb}-DBT** :

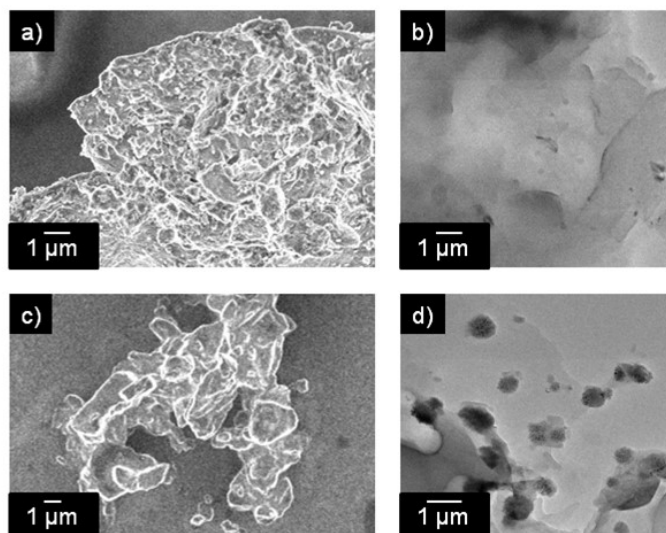


Figure S16. (a,b) Scanning electron microscopic and transmission electron microscopic images of **P_{Fb}-DBT** and $[\text{H}_2\text{P}_{\text{Fb}}\text{-DBT}]^+\text{Cl}^-$ aggregates were drop-casted from methanol solution at 25 °C.

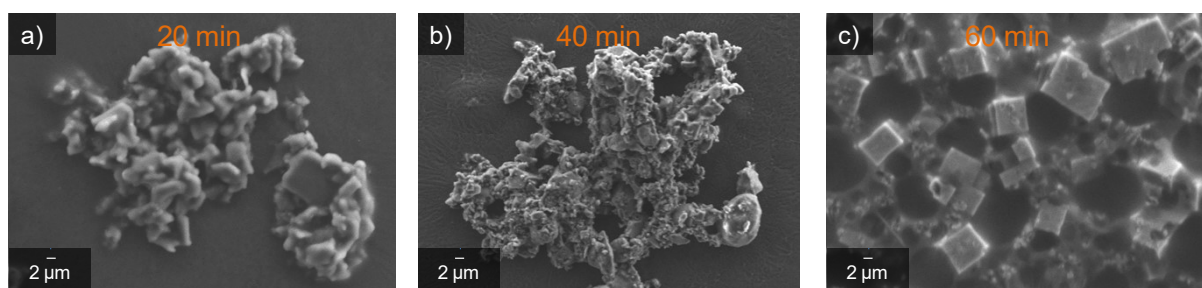


Figure S17. (a-d) Scanning electron microscopic images of light illuminated **P_{Fb}-DBT** aggregates were drop-casted from methanol solution at different time intervals of light illumination in chloroform.

10. Electrochemical Impedance analysis of $\text{P}_{\text{Fb}}\text{-DBT}$ and $\text{P}_{\text{Cu}}\text{-DBT}$ at before and light illuminations conditions:

10.1. Electrochemical Impedance analysis of before and after light illuminated $\text{P}_{\text{Fb}}\text{-DBT}$:

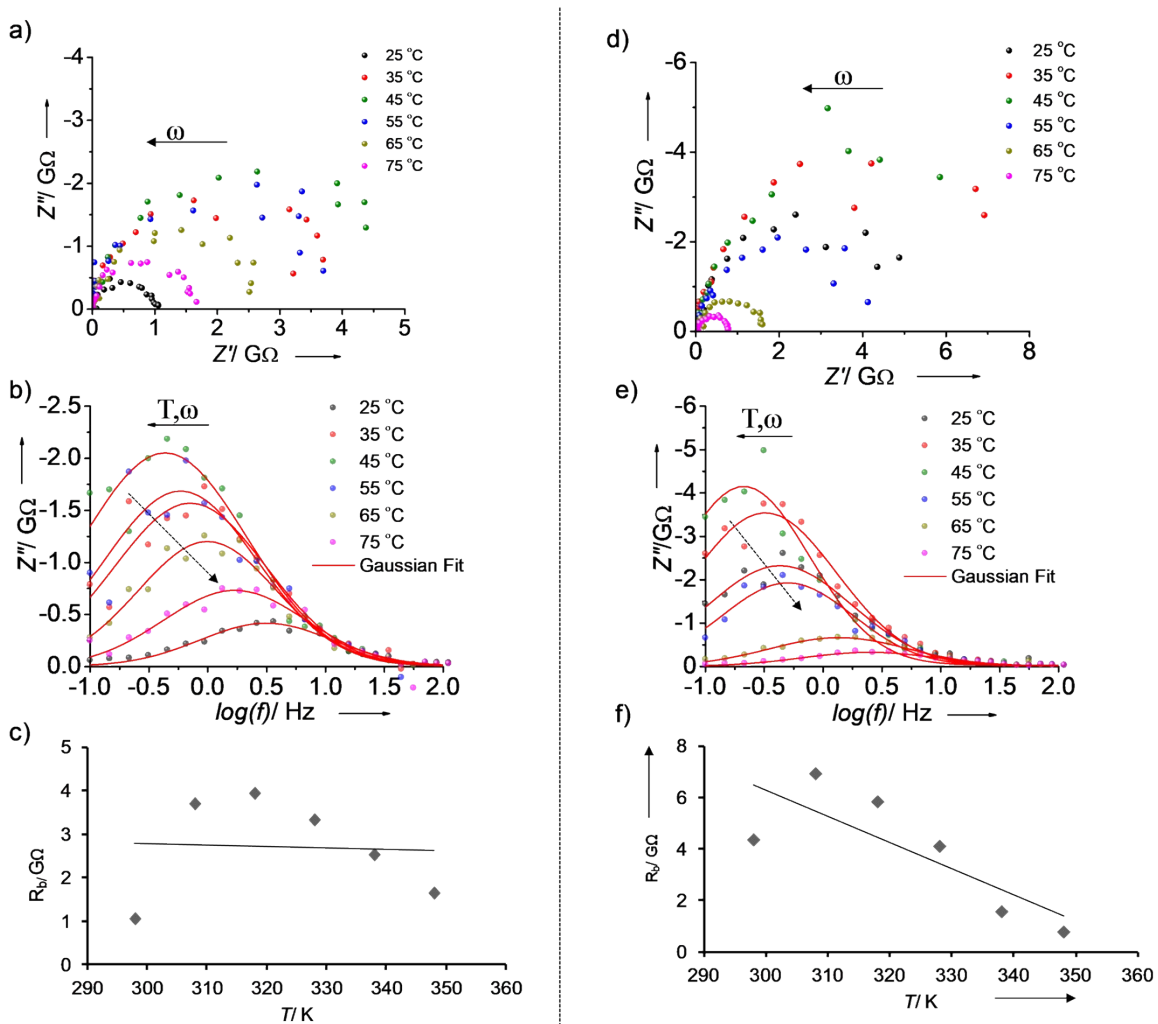


Figure S18. Electrochemical impedance spectral data of $\text{P}_{\text{Fb}}\text{-DBT}$. (a,d) Temperature dependent Nquist plot of before and after light illuminated $\text{P}_{\text{Fb}}\text{-DBT}$ from 25 °C to 75 °C (b,e) Corresponding temperature dependent changes of logarithmic frequency vs Imaginary impedance. (c,f) Plot represents the temperature in Kelvin against bulk resistance at both conditions to determine the electronic and ionic conduction mechanism.

10.2. Electrochemical Impedance analysis of $\text{P}_{\text{Cu}}\text{-DBT}$:

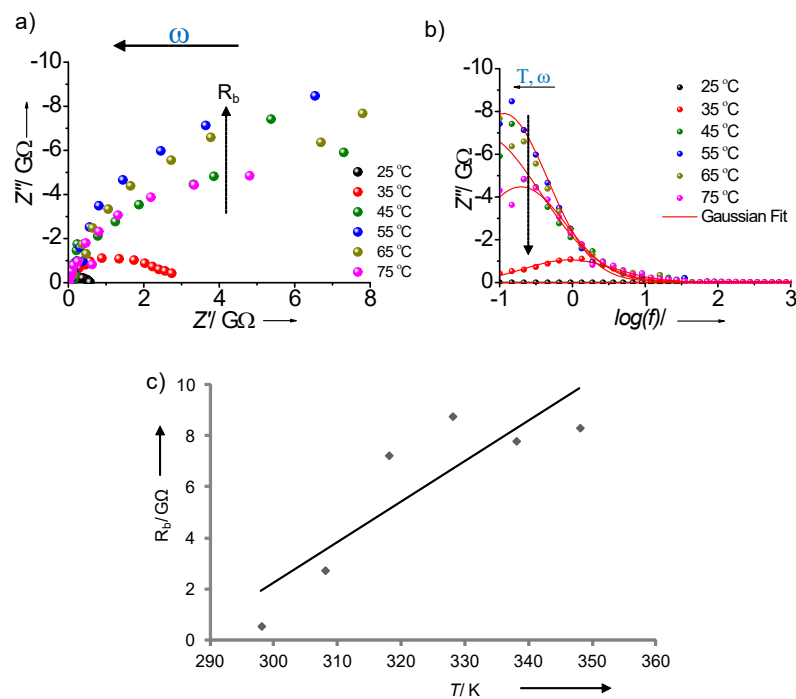


Figure S19. Electrochemical impedance spectral data of $\text{P}_{\text{Cu}}\text{-DBT}$: (a) Nquist plot with variable temperature from 25 °C to 75 °C. (b) Corresponding temperature dependent changes of logarithmic frequency vs Imaginary impedance. (c) Plot represents the bulk resistance against temperature.

10.3. Electrochemical Impedance analysis of light illuminated $\text{P}_{\text{Cu}}\text{-DBT}$:

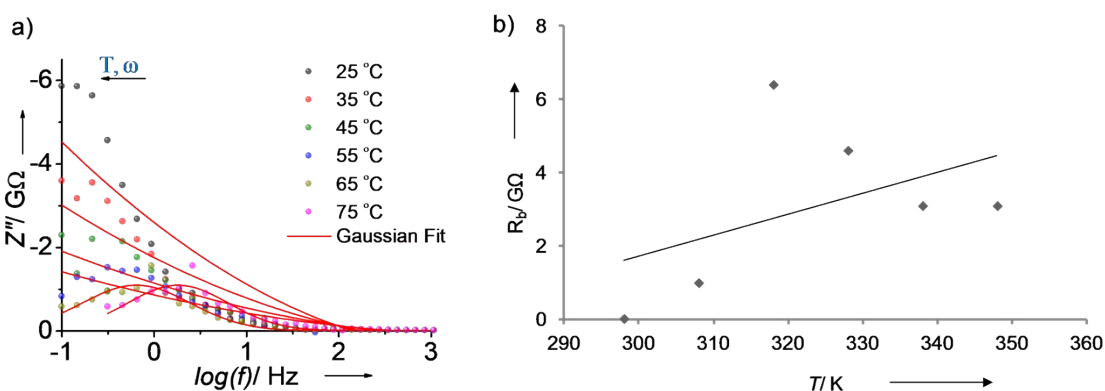


Figure S20. a) Temperature-dependent changes of logarithmic frequency vs Imaginary impedance. b) plot of bulk resistance against the increase in temperature from 25 °C to 75 °C (298 – 348 K) of light-illuminated $\text{P}_{\text{Cu}}\text{-DBT}$.

10.4. Summary of electrochemical impedance data of P_{Fb} -DBT and P_{Cu} -DBT:

Table S2. Electrochemical impedance spectroscopy data of P_{Fb} -DBT and P_{Cu} -DBT; where, R_b = bulk resistance; f_b = bulk frequency, σ = specific conductivity, C_b = bulk capacitance and τ_b = the bulk relaxation time and estimated for the samples at variable temperatures.(^{*} represents light illuminated condition)

Samples	T (K)	R_b (GΩ)	f_b (MHz)	$\sigma \times 10^{-3}$ (S/cm)	C_b (fF)	τ_b (μs)
P_{Fb}-DBT						
	298	1.1	1.04	0.09	1.0	1.529
	308	3.7	2.54	0.03	0.2	0.626
	318	3.9	4.03	0.02	0.1	0.394
	328	3.3	3.20	0.03	0.2	0.497
	338	2.5	2.57	0.04	0.3	0.618
	348	1.6	2.03	0.06	0.5	0.782
P_{Fb}-DBT*						
	298	4.8	4.01	0.02	0.08	0.396
	308	6.9	4.48	0.01	0.05	0.355
	318	5.8	5.04	0.02	0.05	0.316
	328	4.1	4.01	0.03	0.10	0.396
	338	1.5	1.79	0.06	0.60	0.885
	348	7.6	1.61	0.01	1.0	0.989
P_{Cu}-DBT						
	298	0.5	7.97	0.17	0.40	0.199
	308	2.7	1.20	0.03	0.50	1.325
	318	7.2	2.20	0.013	0.09	0.721
	328	8.7	7.96	0.01	0.02	0.200
	338	7.8	7.94	0.012	0.03	0.201
	348	8.3	6.35	0.01	0.03	0.250
P_{Cu}-DBT*						
	298	0.0002	2.53	38.0	252.0	0.628
	308	0.1	1.62	0.09	1.0	0.980
	318	6.4	7.73	0.01	0.03	0.205
	328	4.6	0.64	0.02	0.05	0.249
	338	3.0	0.64	0.03	0.08	0.249
	348	3.1	5.03	0.03	0.10	0.316